Hexatic smectic phase with algebraically decaying bond-orientational order

Lorenzo Agosta,[1] Alfredo Metere,[2,*] and Mikhail Dzugutov[3]
[1]*Department of Materials and Environmental Chemistry, Stockholm University, Svante Arrhenius Väg. 16C, S-10691 Stockholm, Sweden*
[2]*International Computer Science Institute, 1947 Center St., Berkeley, California 94704, USA*
[3]*Royal Institute of Technology, SE-10044 Stockholm, Sweden*

(Received 25 September 2017; revised manuscript received 27 March 2018; published 10 May 2018)

The hexatic phase predicted by the theories of two-dimensional melting is characterized by the power-law decay of the orientational correlations, whereas the in-layer bond orientational order in all the hexatic smectic phases observed so far was found to be long range. We report a hexatic smectic phase where the in-layer bond orientational correlations decay algebraically, in quantitative agreement with the hexatic ordering predicted by the theory for two dimensions. The phase was formed in a molecular dynamics simulation of a one-component system of particles interacting via a spherically symmetric potential. The present results thus demonstrate that the theoretically predicted two-dimensional hexatic order can exist in a three-dimensional system.

DOI: 10.1103/PhysRevE.97.052702

I. INTRODUCTION

The theory of two-dimensional (2D) melting by Kosterlitz, Thouless, Halperin, Nelson and Young (KTHNY) [1] predicts the existence of a distinct new phase intervening between a solid and a liquid. This phase, called hexatic, is a 2D fluid characterized by a quasi-long-range bond orientational order (BOO) (decaying as power law) and short-range (exponentially decaying) positional correlations. The hexatic phase predicted by the KTHNY theory has been observed in a number of real 2D systems [2], but the attempts to find it in three-dimensional (3D) systems have so far been unsuccessful. Nevertheless, its terminology has been carried over to 3D liquid crystals [3] to describe the bond-ordered liquid states found in the axially stacked layers of some smectic liquid crystals [4–6]. These smectic phases, called hexatic smectics, were thus suggested to be the 3D analog of the 2D hexatic phase conjectured by the KTHNY scenario [7]. It has to be stressed, however, that this analogy is purely heuristic. The principal difference between the two phases is that the hexatic smectics exhibit true long-range in-layer BOO in contrast to its power law decay in the 2D hexatic phases. This difference was tentatively attributed to the interaction between the smectic layers and the effect of anisotropic forces [7], but the nature and the origin of the long-range BOO in the hexatic smectic phases still elude comprehensive understanding.

Particle simulations have been actively used to understand the formation mechanism of the smectic liquid crystals in terms of the molecular-level properties [8]. Following the seminal work of Onsager [9], it was commonly believed that formation of smectic phases is driven by the packing entropy of anisometric (rodlike) mesogenic molecules [10]. Accordingly, a rodlike particle shape was assumed in the computer models of smectic phases [11,12]. However, to our knowledge, no unconstrained simulation of a hexatic smectic phase has so far been reported [13].

Two questions of general conceptual interest arise in this context: (1) Is the anisometry of the mesogenic molecules a prerequisite for producing a smectic mesophase and, in particular, a hexatic smectic phase? (2) Can the true long-range BOO observed in the hexatic smectic phases be related to the specific shape of their constituent molecules and the anisotropy of the intermolecular forces?

In this article, we report a molecular-dynamics simulation addressing these questions. It is demonstrated that a single-component system of particles interacting via a spherically symmetric potential forms an equilibrium hexatic smectic mesophase where the in-layer BOO decays as a power law, in quantitative agreement with the KTHNY theory prediction.

II. MODEL AND SIMULATION

We investigated a molecular-dynamics model of 50 000 identical particles confined to a cubic box with periodic boundary conditions interacting via the pair potential shown in Fig. 1. The functional form of the potential energy for two particles separated by the distance r is

$$V(r) = a_1(r^{-m} - d)H(r,b_1,c_1) + a_2 H(r,b_2,c_2), \quad (1)$$

$$H(r,b,c) = \begin{cases} \exp\left(\frac{b}{r-c}\right) & r < c \\ 0 & r \geqslant c \end{cases}. \quad (2)$$

The values of the parameters are presented in Table I. The simulation reduced units are those used in the definition of the potential.

This pair potential represents a modification of an earlier reported one [14] that was found to produce a Cr-B crystalline phase. The main difference between the two potentials is that in the present one the long-range repulsion is extended to a significantly larger distance. In that earlier simulation the latter parameter was found to determine the interlayer spacing.

*alfredometere2@gmail.com

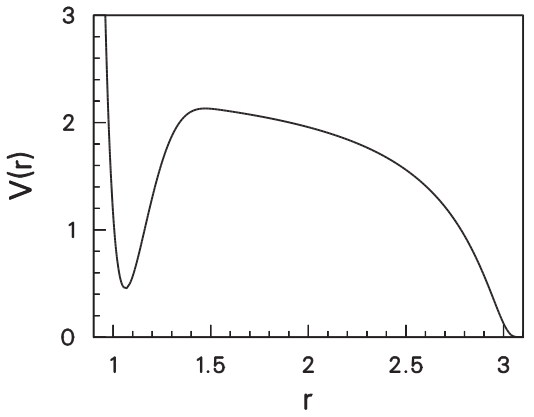

FIG. 1. Pair potential.

III. RESULTS

The system's phase behavior was investigated at a constant number density $\rho = 0.41$. The temperature was changed in a stepwise manner, performing a comprehensive equilibration after each step which typically amounted to 10^7 time steps. The simulation started by equilibrating an isotropic liquid state at sufficiently high temperature $T = 3.0$. Figure 2 shows system's energy and pressure as functions of temperature. Upon cooling, both quantities exhibited a discontinuity at $T = 1.15$, followed by another one at $T = 0.95$. The latter was accompanied by a sharp drop in the diffusion rate (Fig. 2 inset) indicating the formation is a solid state; this was identified as a Cr-B crystalline phase (Fig. 3). Upon reheating, the described temperature variations of the pressure and energy were reproduced. Each observed singularity was found to be accompanied by a hysteresis, a signature of the first-order nature of the respective transition.

The observed phase behavior thus demonstrates the existence of a distinct equilibrium fluid phase interposed between the isotropic liquid and the Cr-B crystalline phase, separated from each of the latter two phases by a first-order transition. The general view of its instantaneous configuration presented in Fig. 4 suggests that this is a smectic liquid crystal composed of uniaxially stacked layers with a liquid-like in-layer diffusion (Fig. 2 inset). We note that its estimated interlayer spacing is consistent with the long-range repulsion distance of the pair potential (Fig. 1).

In order to understand the exact nature of this smectic mesophase we performed a detailed analysis of its in-layer structure. As a first step in the structure characterization we calculated the structure factor $S(\mathbf{Q})$ representing the scattered intensity in the diffraction experiments. It is defined as

$$S(\mathbf{Q}) = \langle \rho(\mathbf{Q})\rho(-\mathbf{Q}) \rangle \tag{3}$$

TABLE I. Values of the parameters for the pair potential used in this simulation [Eq. (1), Fig. 1].

m	a_1	b_1	c_1	a_2	b_2	c_2	d
12	113	2.8	1.75	2.57	0.3	3.1	1.4

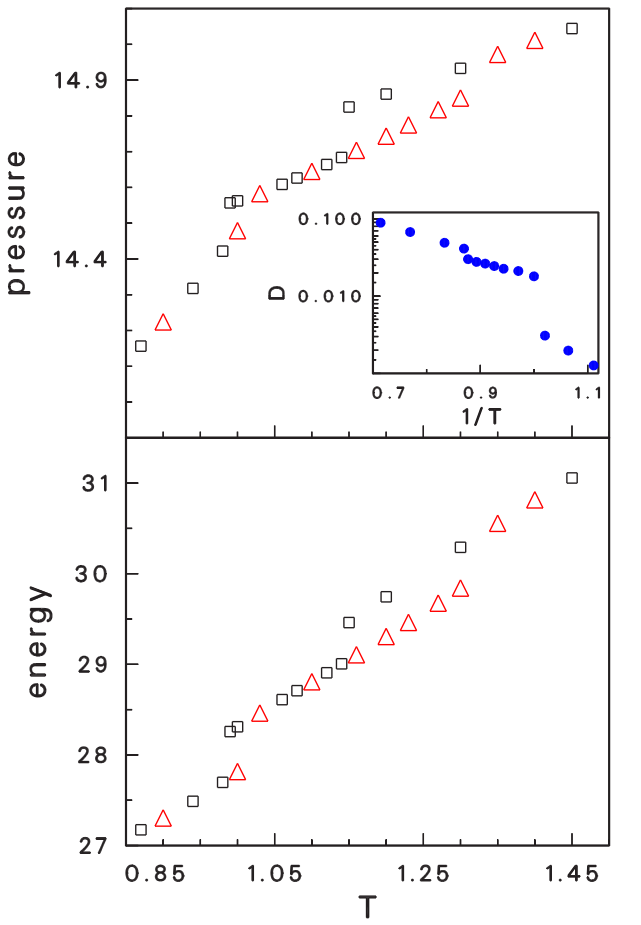

FIG. 2. Temperature variation of the pressure and energy at the number density $\rho = 0.41$. Squares: cooling; triangles: heating. Inset: The Arrhenius plot of the diffusion coefficient.

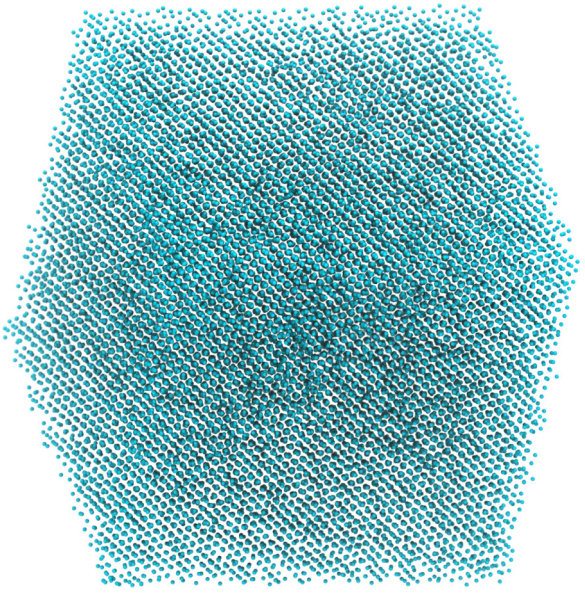

FIG. 3. An axial view of the Cr-B crystal formed as a result of the phase transition upon cooling, at $T = 0.8$. The sixfold positional symmetry of the configuration is apparent.

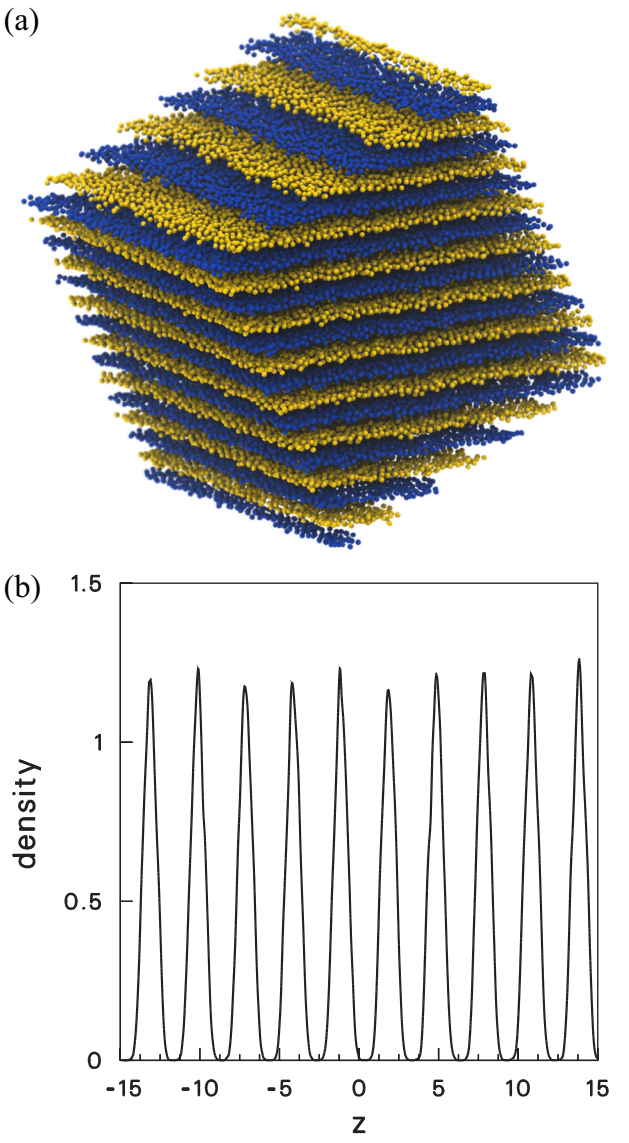

FIG. 4. (a) A view of the simulated smectic phase, adjacent layers are discriminated by shade. (b) The axial density variation in the simulated hexatic smectic phase configuration at $T = 1$. The interlayer distance is consistent with the long-range repulsion distance of the pair potential.

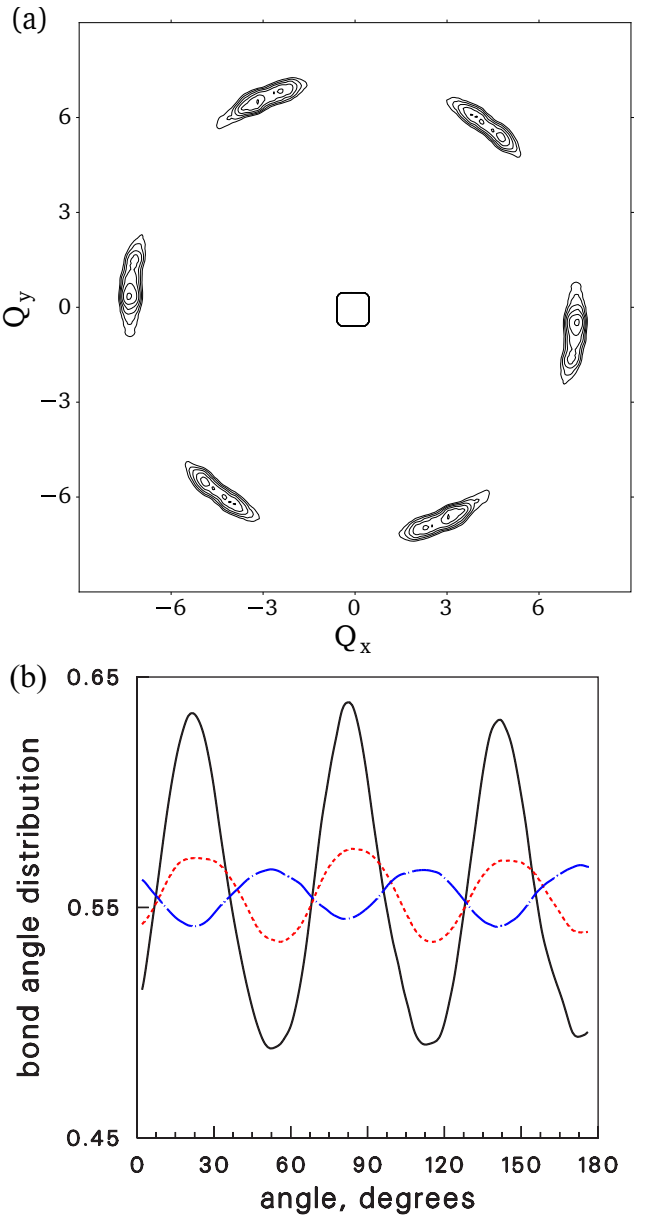

FIG. 5. (a) $S(\mathbf{Q})$ of a single layer calculated in the layer plane, presented by isointensity contours. The lowest level contour corresponds to $S(\mathbf{Q}) = 3.4$, the increment is 0.3. (b) Bond angle distribution. Solid line and dash-dotted line, respectively: one layer at $T = 1.0$ and at $T = 1.1$. Dashed line: entire system, $T = 1.0$.

where $\rho(\mathbf{Q})$ is the $\mathbf{Q}$ component of the spatial Fourier transform of the instantaneous number density distribution of a system of N particles:

$$\rho(\mathbf{Q},t) = \frac{1}{\sqrt{N}} \sum_{k=1}^{N} \exp[-i\mathbf{Q}\mathbf{r}_k], \tag{4}$$

$\mathbf{r_k}$ being the position of particle k, and $\langle\ \rangle$ denoting ensemble averaging.

A spherically averaged static structure factor can be calculated from the spherically invariant radial distribution function $g(r)$ as

$$S(Q) = 1 + 4\pi\rho \int_0^\infty [g(r) - 1] \frac{\sin(Qr)}{Qr} r^2\, dr. \tag{5}$$

As a first step in the structure analysis, we calculated the $S(\mathbf{Q})$ intensity pattern on the reciprocal-space sphere of the radius corresponding to the position of the prominent peaks of the spherically averaged structure factor. This made it possible to determine the global symmetry of the configuration and the axis orientation.

Having established the global uniaxial symmetry of the configuration and the axis orientation, we then calculated $S(\mathbf{Q})$ in the layer plane $Q_z = 0$, Q_z being the axis coordinate. Figure 5(a) shows $S(\mathbf{Q})$ for a single layer averaged over 10^4 time steps. It exhibits a pronounced azimuthal modulation in the form of six diffuse arcs characteristic of the diffraction

patterns of hexatic smectic phases. Their radial position can be identified as $Q = 4\pi/(a\sqrt{3})$ where $a = 0.99$ is the estimated in-layer nearest neighbor distance. We notice that this distance is in good agreement with the position of the first potential minimum (Fig. 1). In this way, the short repulsion and the long repulsion parts of the pair potential act, respectively, as the length and the diameter of the mesogenic molecules forming the real smectic phases: the former define the interlayer particle packing, whereas the latter define the interlayer spacing.

The sixfold angular symmetry of the diffraction pattern is a necessary but not sufficient condition for identifying the simulated phase as a hexatic smectic. To get further evidence for the hexatic nature of its in-layer structure we calculated the bond-orientation distribution, which is shown in Fig. 5(b). The bonds were defined as the pairs of particles within a layer separated by the nearest-neighbor distance a as indicated above. The angles presented in the statistics were measured between the bonds and an axis chosen in the layer plane. The statistics was calculated for an ensemble of configurations produced within a simulation run of 10^4 time steps. The bond angle distribution for a single layer at $T = 1.0$ demonstrates a pronounced sixfold modulation with the amplitude consistent to that observed in the azimuthal variation of $S(\mathbf{Q})$ [Fig. 5(a)]. The amplitude of the distribution modulation for the same layer at $T = 1.1$ is significantly smaller, as well as the one calculated for the entire system.

Next, we analyze the pattern of the local sixfold BOO in a layer configuration. For each particle position $\mathbf{r}_j$ we calculated a vector

$$\Psi(\mathbf{r}_j) = \frac{1}{N_k}\sum_{k=1}^{N_k} e^{i6\theta_{jk}}, \tag{6}$$

where θ_{jk} is the angle formed by the bond linking particle j with its nearest neighbor k relative to an arbitrary axis, and N_k is the number of the nearest neighbors. Figure 6(a) shows the distribution of these vectors in a layer at $T = 1.0$. Each vector $\Psi(\mathbf{r_j})$ is represented by a dot; the dot's size is proportional to $|\Psi(\mathbf{r_j})|$, and the vector orientation is indicated by the dot's color, according to the scale. The distribution exhibits an apparent domain structure. A cluster of coherent hexagonal order percolates through the entire layer, which can account for the sixfold symmetry breaking both in the diffraction pattern and in the bond-angle distribution. In addition, there are twinning domains of hexagonal order rotated by 30° and 15° with respect to the main domain. These domains can also be discerned in the pattern of bonds produced for the same particle of a layer configuration Fig. 7.

The identifying feature of the hexatic phase according to the KTHNY theory is the algebraic decay of its BOO. The latter can be quantified as

$$g_6(r) = \frac{\left\langle \sum_{k\neq j}^{N} \Psi(\mathbf{r}_j)\Psi(\mathbf{r}_k)\delta(r - |\mathbf{r}_j - \mathbf{r}_k|)\right\rangle}{\left\langle \sum_{k\neq j}^{N} \delta(r - |\mathbf{r}_j - \mathbf{r}_k|)\right\rangle}, \tag{7}$$

where N is the number of particles, and angle brackets denote ensemble averaging with respect to all particles. Figure 6(b) shows $g_6(r)$ calculated for an ensemble of configurations of a single layer produced in a simulation run of 10^4 time steps. It is compared with the radial distribution function $g(r)$ [15]

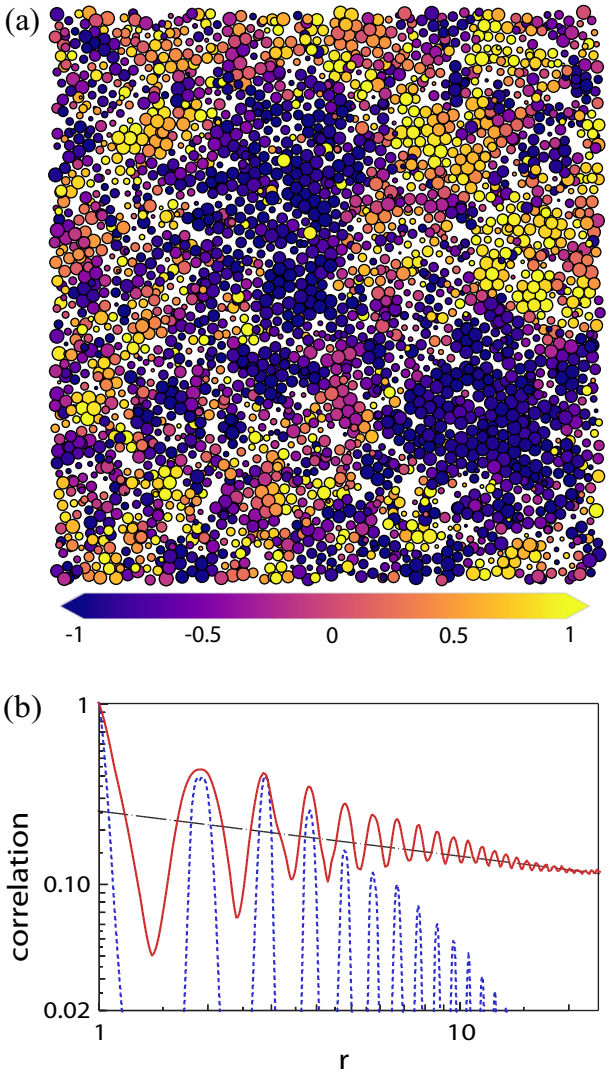

FIG. 6. (a) The local BOO distribution in a layer at $T = 1$. Each dot represents a particle; the size of the dot representing particle j is proportional to $|\Psi(\mathbf{r}_j)|$; its shade indicates $\mathrm{Re}[\Psi(\mathbf{r}_j)]$ according to the scale. (b) Solid line: BOO correlation function $g_6(r)$; dashed line: $g(r) - 1$, both at $T = 1$; dash-dotted line: an asymptotic power-law fit.

expressing the decay of the positional correlation. We find that the calculated $g_6(r)$ asymptotically decays as a power law, in agreement with the prediction of the KTHNY theory for the 2D hexatic [1], whereas $g(r)$ decays exponentially. These results explicitly prove that the layers of the simulated smectic represent 2D hexatic phases as defined by the theory.

It is common to evaluate the degree of hexatic order in the experimentally studied hexatic smectic phases using the BOO parameter defined as

$$C_6 = \left\langle \frac{1}{N}\left|\sum_{i}^{N} \Psi_6(r_i)\right|\right\rangle. \tag{8}$$

We have calculated this parameter within the same layer for which we calculated $g_6(r)$ that was shown in Fig. 6, as a function of temperature. Angle brackets denote averaging over

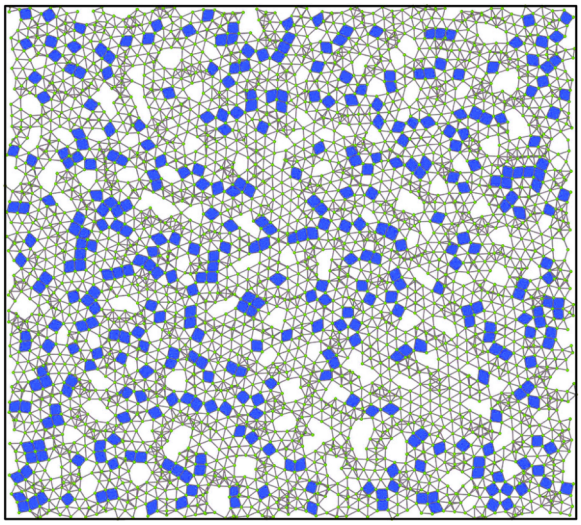

FIG. 7. The pattern of the nearest-neighbor bonds in a layer. There are discernible domains of coherently oriented local hexagonal order. Another prominent element of the pattern are the squares (filled in the plot) which provide the mutual 30° rotation of the apparently twinning hexagonally ordered domains.

the ensemble of configurations produced within the simulation run of 10 000 time steps. The results are presented in Fig. 8.

Figure 9 presents a layer configuration highlighting the variations in the particle positions in the third dimension perpendicular to the layer plane. The results demonstrate that vast majority of the particles remain within a narrow layer with their axial coordinates deviating from the layer plane by not more than $0.4a$, a being the closest interparticle distance within the layer as defined above. The remaining particles deviate from the layer plane within the margin of $0.9a$. These results are apparently consistent with the axial variation of the particle density shown in Fig. 4.

In order to investigate the anisotropy of the particle diffusion in the hexatic smectic phase we separately calculated its axial

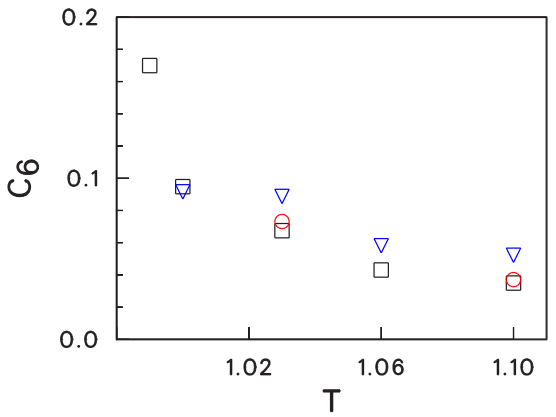

FIG. 8. BOO parameter C_6 of a layer as a function of temperature averaged over the ensemble of configurations produced within the simulation run of 10 000 time steps. Squares and triangles, respectively: cooling and heating of the hexatic formed from the isotropic liquid state. Circles: the hexatic phase formed by melting the Cr-B crystalline phase.

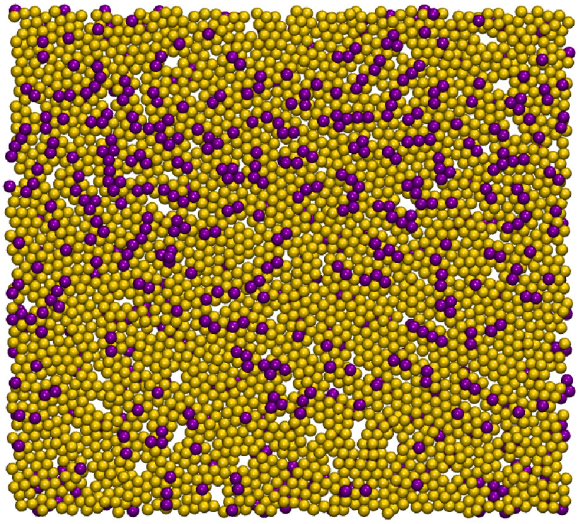

FIG. 9. The particle configuration of the layer shown in Fig. 7. The axial coordinates z_i of the light shaded particles are within the interval $|z_i - z_0| < 0.4a$, z_0 being the average axial coordinate of the particles of the layer, a being the closest interparticle distance within the layer. Darker shaded particles: $0.4a < |z_i - z_0| < 0.9a$.

component $D_\perp$ and the intralayer component $D_\parallel$. It is found that the ratio of these two components is generally temperature independent within the temperature range where the hexatic smectic phase was observed, and it is about $D_\perp/D_\parallel \approx 0.5$. Assuming that the intralayer diffusion is dominated by the particle hopping to the interstitial positions of the local hexagonal configurations, the ratio of the interlayer hopping frequency to that of the intralayer hopping can be estimated as ≈ 0.016. This result is consistent with the result of the experimental measurements on a hexatic smectic phase where the frequency of the interlayer jumps was found to be about 100 times lower than the frequency of the intralayer jumps [16].

In order to establish the exact low-temperature boundary of the simulated hexatic smectic phase at $\rho = 0.41$, we cooled it to the temperature $T = 0.98$ where it was observed to lose its stability with respect to the crystalline phase. Following the process of crystallization at that temperature, we interrupted it after 700 000 time steps at the stage of partial crystallization which was discerned from the energy reduction. This partially crystallized state was then heated to two higher temperatures, $T = 0.99$ and $T = 1$. The energy evolution shown in Fig. 10 demonstrates that at $T = 0.99$ the crystallization process continued, whereas at $T = 1$ the hexatic smectic phase has been restored. This result demonstrates that $T = 0.99$ belongs to the stable crystal domain, while at $T = 1$ the hexatic smectic phase is stable with respect to crystallization.

IV. DISCUSSION

Three conceptually significant aspects of this study deserve to be remarked upon.

First, the finding that a system of identical particles interacting via a spherically symmetric potential can form a hexatic smectic phase changes the basic model of smectic phases, thereby advancing our understanding of the causes underlying the occurrence of particular structures in the phase transformations of liquid crystals.

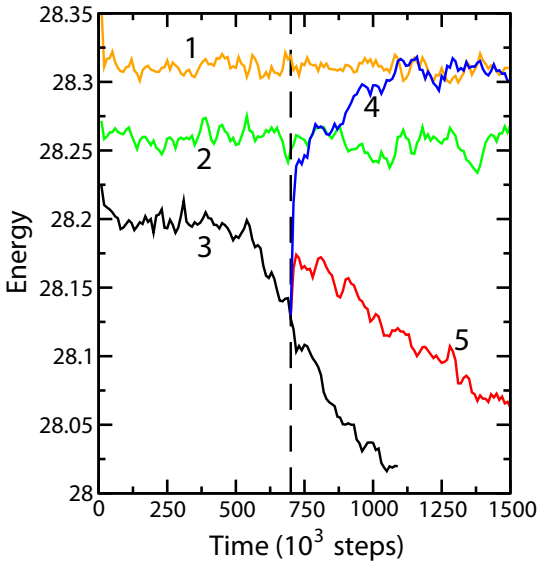

FIG. 10. 1 and 2, respectively: equilibrium states of the hexatic smectic phase at $T = 1$ and $T = 0.99$ produced by cooling. 3: crystallization process in the smectic hexatic phase cooled to $T = 0.98$. 4 and 5, respectively: the results of the heating of the hexatic smectic phase partially crystallized at $T = 0.98$ to $T = 1$ and $T = 0.99$. The dashed vertical line indicates the moment of time when the heating was started.

Second, the observed algebraic power-law decay of the in-layer BOO in a hexatic smectic phase formed by a system of particles with spherically symmetric interaction suggests that the true long-range BOO that has so far been found in the hexatic smectics can be attributed to the rodlike shape of their constituent molecules and the anisotropy of the intermolecular forces.

Third, the hexatic phase predicted by the KHTNY theory of 2D melting has so far not been found to our knowledge in a 3D system. The smectic phase we report here demonstrates the in-layer hexatic order that quantitatively agrees with the theory's prediction. This is an indication that the theory's application scope can include 3D systems.

We note that the pair potential we report is similar to that predicted for colloidal systems [17] (amended with steric repulsion) suggesting that a hexatic smectic phase can be formed by spherical colloidal particles with an appropriately tailored interaction, as microgels or through a cosolute [18].

V. CONCLUSION

In summary, we report a hexatic smectic phase formed in a molecular dynamics simulation of a one-component system of particles interacting via a spherically symmetric potential. In contrast to the hexatic smectics observed so far, its BOO decays algebraically in quantitative agreement with the KTHNY theory prediction for the 2D hexatic phase. The present results thus demonstrate that the theoretically predicted two-dimensional hexatic order can also exist in a three-dimensional system.

ACKNOWLEDGMENTS

We thank Dr. Babak Sadigh and Prof. Francesco Sciortino for illuminating suggestions. GROMACS was used for simulations.

[1] J. M. Kosterlitz and D. J. Thouless, J. Phys. C **5**, L124 (1972); **6**, 1181 (1973); B. I. Halperin and D. R. Nelson, Phys. Rev. Lett. **41**, 121 (1978); D. R. Nelson and B. I. Halperin, Phys. Rev. B **19**, 2457 (1979); A. P. Young, *ibid.* **19**, 1855 (1979).

[2] B. K. Clark, M. Casula, and D. M. Ceperley, Phys. Rev. Lett. **103**, 055701 (2009); A. H. Marcus and S. A. Rice, *ibid.* **77**, 2577 (1996).

[3] P.-G. de Gennes and J. Prost, *The Physics of Liquid Crystals* (Clarendon Press, Oxford, 1993).

[4] W. H. de Jeu, B. I. Ostrovskii, and A. N. Shalaginov, Rev. Mod. Phys. **75**, 181 (2003).

[5] J. W. Goodby, M. A. Waugh, S. M. Stein, E. Chin, R. Pindak, and J. S. Patel, Nature (London) **337**, 449 (1989).

[6] I. A. Zaluzhnyy, R. P. Kurta, E. A. Sulyanova, O. Yu. Gorobtsov, A. G. Shabalin, A. V. Zozulya, A. P. Menushenkov, M. Sprung, A. Krowczynsky, E. Gorecka, B. I. Ostrovskii, and I. A. Vartanyants, Soft Matter **13**, 3240 (2017).

[7] R. J. Birgeneau and J. D. Lister, J. Phys. (Paris), Lett. **39**, 399 (1978); J. Prost, Adv. Phys. **33**, 1 (1984).

[8] M. Wilson, Int. Rev. Phys. Chem. **24**, 421 (2005); C. M. Care and C. J. Cleaver, Rep. Prog. Phys. **68**, 2665 (2005).

[9] L. Onsager, Ann. N.Y. Acad. Sci. **51**, 627 (1949).

[10] T. C. Lubensky, Solid State Commun. **102**, 187 (1997).

[11] P. Bolhuis and D. Frenkel, J. Chem. Phys. **106**, 666 (1997).

[12] E. de Miguel, E. M. del Rio, and F. J. Blas, J. Chem. Phys. **121**, 11183 (2004).

[13] B. Martinez-Haya and B. Cuetos, J. Phys. Chem. B **111**, 8150 (2007); K. M. Aoki, M. Yoneya, and H. Yokoyama, Phys. Rev. E **81**, 021701 (2010).

[14] A. Metere, T. Oppelstrup, S. Sarman, A. Laaksonen, and M. Dzugutov, Phys. Rev. E **88**, 062502 (2013).

[15] J.-P. Hansen and I. R. McDonald, *Theory of Simple Liquids*, 2nd ed. (Academic Press, New York, 1990).

[16] S. Žumer and M. Vilfan, Phys. Rev. A **28**, 3070 (1983).

[17] E. J. Verwey, and J. T. G. Overbeek, *Theory of the Stability of Lyophobic Colloids* (Elsevier, Amsterdam, 1948); J. N. Israelachvili, *Intermolecular and Surface Forces*, 3rd ed. (Academic Press, New York, 2011).

[18] N. A. Garcia, N. Gnan, and E. Zaccarelli, Soft Matter **13**, 6051 (2017); N. Gnan, L. Rovigatti, M. Bergman, and E. Zaccarelli, Macromolecules **50**, 8777 (2017).